


 Cite this: *RSC Adv.*, 2018, **8**, 19724

An amperometric glucose biosensor based on PEDOT nanofibers

 Merih Zeynep Çetin and Pınar Camurlu *

Here we present a simple, low cost approach for the production of PEDOT nanofiber biosensors using simple techniques. Firstly, nanofibers of PEDOT were produced by the chemical vapor polymerization of EDOT on FeCl_3 containing electrospun PAN nanofiber mats. The nanofibers were characterized by SEM, FTIR, CV and conductivity studies, which indicated the formation of homogeneous, porous, electroactive PEDOT nanofibers. The fabrication of biosensors was achieved through the loading of various amounts of GOx on the nanofibers. To uncover their capability, the biosensors were operated under both hydrogen peroxide production and oxygen consumption conditions. For each biosensor current response *versus* glucose concentration calibration curves were plotted. The sensitivity, linear range, LOD, K_m and I_{max} values of the biosensors were determined and the stabilities of all the sensors were investigated. The biosensor operating at 0.6 V revealed a lower LOD with a wider linear range, higher stability, good sensitivity and selectivity. For example, the PEDOT-NFs/GOx-3 nanofiber biosensor showed good sensitivity ($74.22 \mu\text{A mM}^{-1} \text{cm}^{-2}$) and LOD ($2.9 \mu\text{M}$) with a response time of 2–3 s without any interference effects. The PEDOT-NFs/GOx-2 biosensor operating at -0.6 V exhibited extreme sensitivity of $272.58 \mu\text{A mM}^{-1} \text{cm}^{-2}$. Our studies have shown that having good sensitivity, LOD and stability makes these interference-free, easy to construct sensors viable candidates for commercialization.

 Received 13th February 2018
 Accepted 4th May 2018

DOI: 10.1039/c8ra01385c

rsc.li/rsc-advances

Introduction

Nanofibers have attracted considerable attention for the construction of sensors owing to their unique properties such as high surface area, flexibility, porosity and their portable nature. In particular, the high surface area of nanofibers makes them useful as large immobilization sites, resulting in an increase in the number of interactions with analytes. Hence, nanofiber-based biosensors are expected to be more sensitive, with a low limit of detection, long shelf life and fast response time for biosensor applications.¹ Day by day, the utilization of nanofibers increase in sensors and their properties could be improved by the use of conducting polymers.

Poly(3,4-ethylenedioxythiophene) (PEDOT), which exhibits high electrical conductivity, long term electrochemical stability, high charge mobility, and a low energy band gap, can be used in many areas. In particular, its use in biosensors is preferred due to its good electroactivity in phosphate buffer.^{2–4} PEDOT is also an excellent material because of its suitability as a matrix for enzyme immobilization and its unique mechanism of direct electron transfer during detection.^{5,6} However, there have been a limited number of reports on biosensor studies with PEDOT nanofibers used for the construction of glucose sensors in the literature. Yang *et al.* have developed an electrochemical

biosensor using PEDOT nanofibers and a PEDOT film. They combined the electrospinning of PLLA/chloroform with the electrochemical polymerization of EDOT to prepare biosensor electrodes. Their results showed that the sensitivity of the biosensor with PEDOT nanofibers is higher than that of the PEDOT film.⁷ Santhosh *et al.* prepared a PEDOT-Pd-GOx nanofiber electrode using a micellar assisted soft template and ionic liquid method. Their results showed that the glucose biosensor exhibits a good linear range and high sensitivity.⁸ Lastly, Hosseini *et al.* reported the use of Pd nanoparticles incorporated inside PEDOT nanofibers as biosensor electrodes. Their results showed that the Pd-PEDOT nanofiber modified electrode has good electrochemical ability for glucose detection in the presence of uric acid and ascorbic acid.⁹ However, all of these studies were limited by the moderate sensitivity of the biosensors, which lie within the range of 1.6 to $24.04 \mu\text{A mM}^{-1} \text{cm}^{-2}$, indicating the need for improvement. A similar argument applies to the LOD values.

Electrospinning is a basic and cheap method for obtaining homogenous nanofibers. Chemical vapor polymerization (CVD) provides a thinner surface coating using smaller monomer quantities with respect to other deposition techniques and it allows preparation without solvent.^{9–11} Contrary to electrochemical polymerization, which is a perfect fit for film preparation, chemical polymerization offers the unique approach of coating every single nanofiber individually. To the best of our knowledge, there have been no reports on the production of

Akdeniz University, Department of Chemistry, 07058, Antalya, Turkey. E-mail:
 pcamurlu@akdeniz.edu.tr



PEDOT nanofibers in combination with electrospinning and chemical vapor polymerization for utilization in glucose detection.

In this work, new amperometric glucose biosensors were generated by the combination of a simple, cost effective electrospinning technique and chemical vapor polymerization. First of all, polyacrylonitrile (PAN) nanofibers were obtained by electrospinning, followed by the chemical vapor polymerization of EDOT monomer in order to obtain conductive PEDOT nanofibers. Lastly, these electrodes were used as a matrix for enzyme immobilization with different GOx enzyme units. To uncover their capability, the biosensors were operated under both hydrogen peroxide production and oxygen consumption conditions. For each biosensor current response (ΔI) *versus* glucose concentrations (mM) calibration curves were plotted. The resulting amperometric measurements were used to calculate the linear range, sensitivity, response time, operational stability, Michaelis–Menten constant (K_m) and limit of detection (LOD) of the generated biosensors. Our results showed that the PEDOT-GOx nanofiber biosensors have good sensitivity, high operational stability, fast response time and the lowest K_m . This novel approach has paved the way for the construction of very cheap, easy to fabricate sensors with very challenging LOD and sensitivity values compared to those in literature, which were prepared using high cost materials and laborious techniques.

Experimental

General

Polyacrylonitrile (PAN, M_w : 150 000 g mol⁻¹), *N,N*-dimethylformamide (DMF, 99%), ferric chloride (FeCl₃), ethanol (99.9%), 3,4-ethylenedioxothiophene (EDOT), glucose oxidase from *Aspergillus niger* (Type X-S, lyophilized powder), glutaraldehyde solution (50 wt% in H₂O) and sodium dodecyl sulfate (SDS) (ACS reagent, $\geq 99.0\%$) were purchased from Sigma-Aldrich and disodium hydrogen phosphate (anhydrous for analysis, Emsure®), sodium dihydrogen phosphate monohydrate (for analysis, Emsure®) and methanol were purchased from Merck. A direct-Q® Water Purification System (Merck Millipore) was used for achieving ultra-pure water. The structural analyses of the PEDOT nanofibers and PAN were investigated using a Bruker Tensor 27 FT-IR spectrometer. Morphological analyses of the PAN nanofibers, PEDOT nanofibers and PEDOT-GOx nanofibers were performed by Zeiss LEO 1430 scanning electron microscopy (SEM). Electrochemical analyses and amperometric measurements were performed using an Ivium Compactstat. Conductivity measurements on 700 nm thick samples were recorded according to the van der Pauws method. High-performance liquid chromatography (HPLC) measurements were made using an Agilent 1100 series HPLC system.

Fabrication of PAN nanofibers

The electrospinning setup consisted of a syringe pump (New Era Pump Systems model no: NE-300, NY, USA) and a DC power

supply (GAMMA model no: ES30P, USA). While the PAN nanofibers were spun on a Pt disk electrode for biosensor fabrication, for the structural and morphological characterization the nanofibers were spun onto aluminum foil. 1 ml h⁻¹, 15 kV and 15 cm were chosen as the optimum electrospinning parameters. A 7 wt% PAN/DMF solution was prepared and the electrospinning process was carried out at room temperature in a plexiglass box.

Fabrication of PEDOT nanofibers

Conductive PEDOT nanofibers were obtained by the chemical vapor polymerization of EDOT.¹² The electrospun PAN nanofibers were dipped into 20 wt% FeCl₃/ethanol, as an oxidant solution. Then, these nanofibers with the oxidant were put into a glass reactor and were exposed to EDOT (100 μ l) vapor under an active vacuum for 15 s and then under a passive vacuum for a desired time (from 5 minutes to 24 hours). After chemical vapor polymerization, these nanofibers were taken from the reactor and left under atmospheric pressure for 1–2 h. Lastly, they were washed with methanol for 15 min and then dried under vacuum at room temperature for 24 h.

Fabrication of PEDOT-GOx nanofiber biosensors

To fabricate PEDOT-GOx nanofiber enzyme biosensors, a predetermined amount of GOx solution (in ultra-pure water) was dropped onto PEDOT nanofibers. After 30 min, the same amount of 1 wt% GA solution (in ultra-pure water) was dropped onto enzyme-containing PEDOT nanofibers and left to dry for another 30 min at room temperature.¹³ Finally, these PEDOT-GOx nanofiber biosensors were kept at 4 °C (in 0.1 M, pH = 7 PBS solution) in a refrigerator. In order to reveal the effect of the enzyme, five different enzyme units, 46.25 U GOx, 92.5 U GOx, 185 U GOx, 277.5 U GOx and 370 U GOx, were used. These biosensors were named: PEDOT-NFs/GOx-1 electrode, PEDOT-NFs/GOx-2 electrode, PEDOT-NFs/GOx-3 electrode, PEDOT-NFs/GOx-4 electrode and PEDOT-NFs/GOx-5 electrode, respectively.

Amperometric response measurements

12 mg SDS/10 ml PBS (0.1 M, pH = 6.5) solution was used as an electrolyte in a three electrode cell configuration, where Ag/AgCl was used as the reference electrode and Pt wire was used as the counter electrode. Amperometric responses were recorded using an Ivium Compactstat while applying 0.6 V or -0.6 V to the working electrode (PEDOT-GOx electrodes). After stabilization of the background current, aliquots of glucose solution were injected into the stirring PBS solution and then current exchanges were recorded against time. At 0.6 V, hydrogen peroxide production and at -0.6 V oxygen consumption followed and the results were directly correlated with glucose concentration. The results were used to calculate the sensitivity, linearity, response time, operational stability, Michaelis–Menten constant (K_m)¹⁴ and limit of detection (LOD) (S/N = 3).¹⁵ The SDS/PBS solution was refreshed and the biosensor was rinsed with ultra-pure water after every measurement.



Results and discussion

Morphology, structural, and electrochemical analyses of the PEDOT nanofibers

Fig. 1 shows the SEM images of the PAN nanofibers, which were achieved through the electrospinning of a 7 wt% PAN/DMF solution. As can be seen, perfectly smooth, bead free, homogenous PAN nanofibers were obtained with an average diameter of around 280 nm. The average diameters of the nanofibers were determined using Image Pro Plus to randomly measure the diameters of 25 individual fibers.

To determine the optimum chemical vapor polymerization conditions, FeCl_3 containing PAN nanofibers was exposed to EDOT monomer for different polymerization periods and the obtained conductive PEDOT mats were analyzed by SEM. As can be seen in Fig. 1, longer exposure periods yielded in formation of higher amounts of PEDOT which led to blocking of PAN nanofibers. Contrary to previous studies,^{12,16} polymerization periods that were longer than 10 min were seen to have an adverse effect, which resulted in the complete loss of nanofiber morphology. Therefore, 5 min was considered to be the optimum polymerization period where the mats showed the characteristic porous structure of PEDOT in a homogeneous nanofiber morphology. When compared with the PAN nanofibers, the average diameter of the PEDOT nanofibers increased to ~ 350 nm (Fig. 1F) and the nanofiber morphology changed.

Fig. 2 shows the comparative FT-IR spectra of the PEDOT nanofibers and PAN powders. As can be seen, PAN showed typical characteristic vibrations at 2940 cm^{-1} for CH stretching, 2240 cm^{-1} for $\text{C}\equiv\text{N}$ stretching and 1448 cm^{-1} for CH_2 stretching. The FT-IR spectrum of the PEDOT nanofibers not only showed the characteristic bands of PEDOT, such as at 1640 cm^{-1} , 1360 cm^{-1} , 1198 cm^{-1} , 1090 cm^{-1} and $850\text{--}960\text{ cm}^{-1}$, but also the characteristic bands of PAN at 2240 cm^{-1} and 2940 cm^{-1} . Among these, the absorption bands at 1640 cm^{-1} and 1360 cm^{-1} were ascribed to the $\text{C}=\text{C}/\text{C}-\text{C}$ stretching vibrations of the thiophene rings. The peaks at 1200 cm^{-1} and 1070 cm^{-1} correspond to the $\text{C}-\text{O}-\text{C}$ stretching

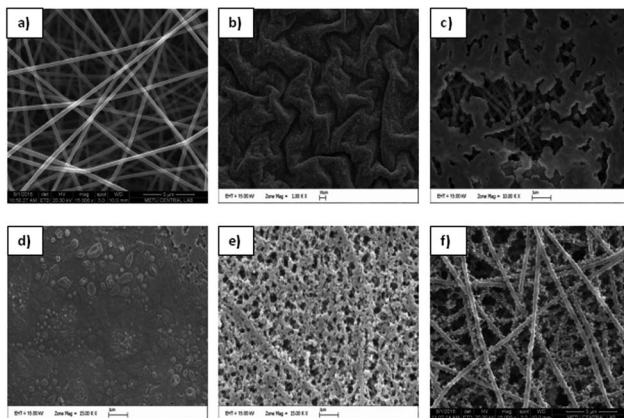


Fig. 1 SEM images of PAN nanofibers (a) and PEDOT nanofibers that were achieved after polymerization periods of (b) 24 h, (c) 3 h, (d) 10 min, (e) 5 min, and (f) 15 min.

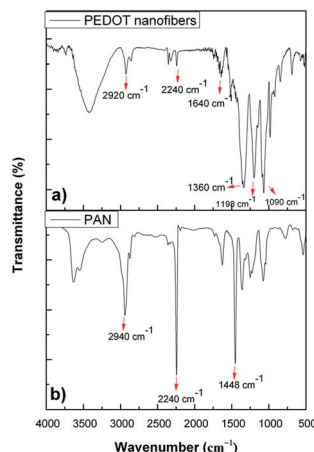


Fig. 2 FTIR spectra of (a) PEDOT nanofibers and (b) PAN powder.

of the etheric bridge of EDOT and the peaks at $850\text{--}960\text{ cm}^{-1}$ are due to the vibrations of the S-C bonds of the PEDOT chains.^{7,17-20} With the presence of typical signals for both EDOT and PEDOT we could conclude that the chemical vapor polymerization of EDOT was achieved and that PEDOT was successfully coated on the surface of the PAN nanofibers.

The electrochemical properties of the PEDOT nanofibers were investigated by cyclic voltammetry. The mats were coated on a Pt disk electrode and scanned between -1 V and $+1.2\text{ V}$ in $0.1\text{ M} \text{NBu}_4\text{PF}_6/\text{ACN}$ at various scanning rates. The PEDOT nanofibers displayed very well-defined oxidation and reduction signals at around $+0.4\text{ V}$ and 0.12 V , respectively.

The redox behavior of the PEDOT nanofibers was in accordance with that observed for simple, chemically synthesized PEDOT²¹⁻²³ and other PEDOT nanofibers.^{12,16} Contrary to the electrochemically synthesized PEDOT, the electrochemical signal of these nanofibers revealed a direct correlation with the square root of the scan rate, which indicates the diffusion controlled nature of the redox process (Fig. 3). Such behavior

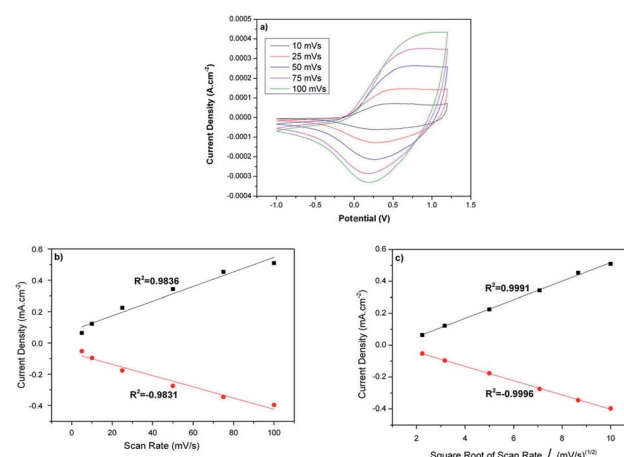


Fig. 3 (a) Cyclic voltammogram of PEDOT nanofibers in $0.1\text{ M} \text{NBu}_4\text{PF}_6/\text{ACN}$ at various scan rates, and plots of the anodic and cathodic peak current densities vs. (b) the scan rate, (c) the square root of the scan rate.

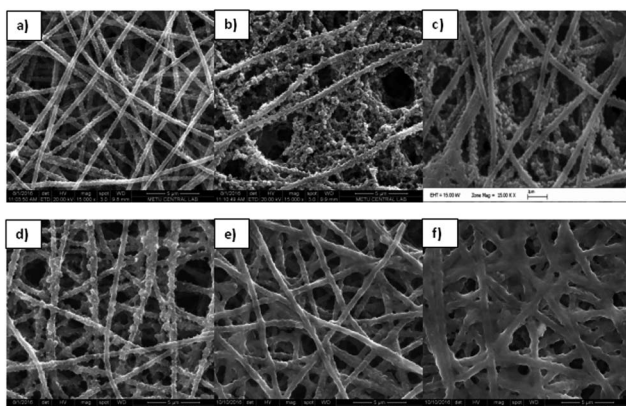


Fig. 4 SEM images of (a) PEDOT nanofibers in phosphate buffer, (b) a PEDOT-NFs/GOx-1 nanofiber mat, (c) a PEDOT-NFs/GOx-2 nanofiber mat, (d) a PEDOT-NFs/GOx-3 nanofiber mat, (e) a PEDOT-NFs/GOx-4 nanofiber mat and (f) a PEDOT-NFs/GOx-5 nanofiber mat. (The magnification is 15 000 \times).

was also reported in previous studies that focused on the characterization of carbon nanofibers with electrochemically deposited PEDOT coatings.^{12,22,24–26}

The collective results from the SEM, FTIR and CV analyses suggest that the prepared mat has a homogeneous, porous, electroactive PEDOT coating on the surface of the PAN nanofibers, which makes it a highly promising candidate for the effective entrapment of enzymes and transfer of electrical signals. The electrical conductivity of the PEDOT nanofiber mat was measured to be 742.9 S cm⁻¹ using the van der Pauw method. To the best of our knowledge, this value is the highest conductivity value that has been recorded for PEDOT nanofibers.^{16,25,27–30}

Fabrication of the biosensors

To fabricate the PEDOT-NFs/GOx nanofiber enzyme biosensors, five different enzyme units were used. Fig. 4 shows the SEM images of the PEDOT nanofibers kept in a buffer solution and

the GOx loaded PEDOT nanofibers. The diameter of the homogeneous PEDOT nanofibers, which were kept in buffer solution, was found to be \sim 425 nm (Fig. 4A), indicating the swelling of the fibers in buffer solution. Acrylic polymers are known to swell and fiber diameters increase when they interact with liquids with a high dipole moment, such as water. Therefore, the increase in the diameter of the PEDOT nanofibers in buffer solution could also stem from the strong plasticizing effects of high dipole moment liquids on the PAN nanofibers.³¹ Fig. 4 shows the morphology of the nanofibers after the loading of different amounts of GOx. As can be seen, the average diameter increased from \sim 425 nm to \sim 780 nm (Table 1) and the nanofibers morphology changed a little upon loading.

Amperometric studies on the PEDOT-NFs/GOx nanofiber biosensors based on hydrogen peroxide production

Some operational parameters, such as the pH value of the buffer solution, the applied potential and amount of enzyme loading can affect the biosensor performance. Therefore, the optimum pH and potential must be determined for biosensor electrodes before the amperometric measurements. For this purpose, buffer solutions at different pH values (in the 5.5–7.5 range) were used in order to determine the optimum pH by measuring the current response to a 0.5 mM glucose solution at 0.65 V. Fig. 5a shows the effect of the pH value on the PEDOT-NFs/GOx biosensors, where the maximum response was determined at a pH of 6.5. Fig. 5b shows the effect of applied potential on the PEDOT-Gox biosensor, where the maximum current response was achieved at 0.6 V, at pH 6.5. Hence, the potential of 0.6 V and pH 6.5 were found to be the optimum conditions for our experiments.

Lastly, in order to determine the optimum enzyme loading, five different enzyme electrodes were prepared and tested for different glucose concentrations under previously determined optimum conditions. All of the amperometric studies were performed in PBS while stirring (200 rpm) under ambient conditions. After the current stabilized, increasing amounts of

Table 1 Performances of all of the PEDOT-NFs/GOx nanofiber biosensors at 0.6 V

	PEDOT-NFs/ GOx-1	PEDOT-NFs/GOx-2	PEDOT-NFs/GOx-3	PEDOT-NFs/GOx-4	PEDOT-NFs/GOx-5
Linear range	0.01–2.5 mM	0.01–1.9 mM and 0.06–5.0 mM	0.01–1.7 mM	0.01–1 mM and 0.1–4.5 mM	0.01–14 mM
Sensitivity (μ A mM ⁻¹ cm ⁻²)	53.58	85.20 and 67.86	74.22	72.61 and 45.67	24.47
LOD (μ M)	7.2	9.6	2.9	4	1.1
Operational stability	After the twelfth use, 80.05%	After the twentieth use, 80.86%	After the twenty fourth use, 93.11%	After the twenty first use, 85.44%	After the twenty fifth use, 87.63%
Std. deviation	\pm 0.1434	\pm 0.0636	\pm 0.0137	\pm 0.039	\pm 0.0164
RSD	17.3%	8.912%	2.96%	5.66%	5.82%
K_m (mM)	2.07	4.28	0.911	4.07	3.197
I_{max} (μ A)	3.97	12.95	2.893	11.24	4.43
Response time (s)	1–2	2–3	2–3	3–4	220
Diameter of the nanofibers (nm)	\sim 435	\sim 575	\sim 620	\sim 700	\sim 780

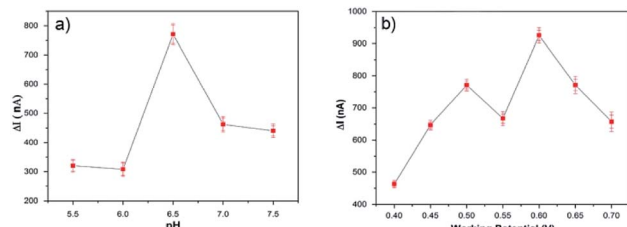


Fig. 5 The effect of (a) pH and (b) potential on the response of the PEDOT-NFs/GOx biosensor to 0.5 mM of glucose, in 0.1 M PBS at 25 °C.

glucose solution were dropped into the stirred PBS solution and the current exchange was recorded. For each biosensor, the current response (ΔI) versus glucose concentrations (mM) calibration curves were plotted and standard deviation values were determined. The sensitivity and linear range values were calculated from calibration graphs for each biosensor. Moreover, the kinetic parameters (K_m and I_{max}) were calculated by means of the Lineweaver–Burk plot. Table 1 shows the performances of the generated biosensors. The biosensors exhibited suitable sensitivity (from $24.47 \mu\text{A mM}^{-1} \text{cm}^{-2}$ to $85.2 \mu\text{A mM}^{-1} \text{cm}^{-2}$) and good LOD (from $1.1 \mu\text{M}$ to $9.6 \mu\text{M}$). Apart from PEDOT-NFs/GOx-1, all of the biosensors preserved $\sim 80\%$ of their activity for up to 20–25 consecutive uses. As seen in Table 1, the optimum biosensor was determined to be the PEDOT-NFs/GOx-3 biosensor, which revealed the highest operational stability, the lowest K_m , the lowest standard deviation, a low LOD and good sensitivity. The biosensor showed the highest sensitivity value and lowest LOD, when compared to the PEDOT based glucose biosensors in literature.^{3,7,8,32}

Amperometric measurements on the PEDOT-NFs/GOx-3 nanofiber biosensor

Fig. 6a shows the amperometric response of the PEDOT-NFs/GOx-3 nanofiber electrode on the successive addition of glucose (from 0.01 mM to 4 mM). The response current increased upon an increase in the glucose concentration and the biosensor became saturated at about 1.7 mM (Fig. 6b). The linear range of the calibration curve was found to be 0.01–1.7 mM and the LOD was found to be $2.9 \mu\text{M}$. The PEDOT-NFs/GOx-3 nanofiber electrode reached a steady state in less than 3 s. This demonstrated the fast electron exchange and good electrocatalytic oxidative behavior of the

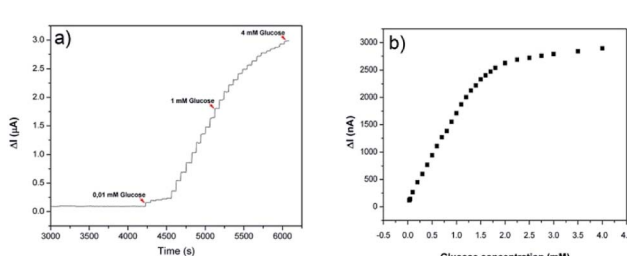


Fig. 6 (a) Amperometric response of the PEDOT-NFs/GOx-3 biosensor to the addition of glucose and (b) the calibration curve of the PEDOT-NFs/GOx-3 biosensor at 0.6 V, pH: 6.5.

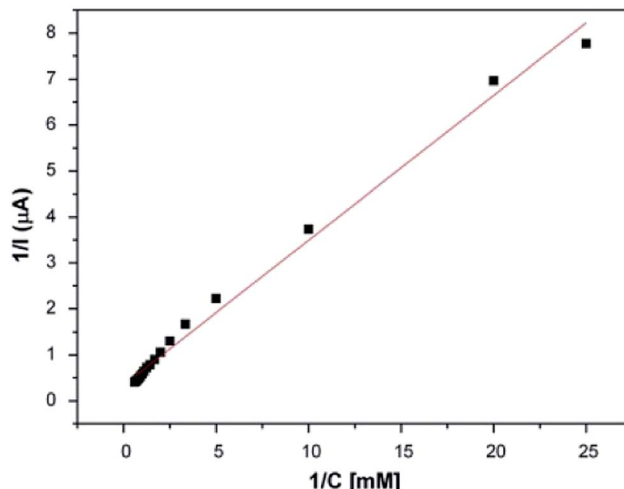


Fig. 7 The Lineweaver–Burk plot of the PEDOT-NFs/GOx-3 biosensor.

nanofibers. The sensitivity of the PEDOT-NFs/GOx-3 biosensor was calculated to be $74.22 \mu\text{A mM}^{-1} \text{cm}^{-2}$, which is the highest value in comparison to other glucose biosensors based on PEDOT nanofibers and films.^{33–35} For instance, Hosseini *et al.*³ and Santhosh *et al.*⁸ both reported on glucose biosensors based on palladium-PEDOT nanofibers where the sensors revealed good but lower sensitivities, such as $24.04 \mu\text{A mM}^{-1} \text{cm}^{-2}$ and $1.6 \mu\text{A mM}^{-1} \text{cm}^{-2}$, respectively. Yang *et al.*⁷ and Layton *et al.*³² on the other hand, reported glucose biosensors of poly(l-lactide)/PEDOT nanofibers with sensitivities of $6.4 \mu\text{A mM}^{-1} \text{cm}^{-2}$ and $5.7 \mu\text{A mM}^{-1} \text{cm}^{-2}$, respectively. A similar conclusion can be drawn when the studies based on polypyrrole nanofibers^{13,36} and polyaniline nanofibers³⁷ are considered. To date, amperometric glucose biosensors based on various nanomaterials have been extensively studied and some critical reviews have been published.^{38,39} Among these, some concentrated on the utilization of carbon nanomaterials of carbon nanotubes (CNTs) and graphene,⁴⁰ nanostructured metal oxides,⁴¹ and silver nanoparticles,⁴² which are known to be high cost materials. From these reviews, with the exception of some of the state-of-the-art performances, the sensitivities reported in this study are highly comparable to those in literature.

As a second step, the kinetic parameters were determined from a Lineweaver–Burk plot. According to Fig. 7, the K_m value was calculated to be 0.911 mM and the I_{max} was found to be $2.893 \mu\text{A}$. In order to examine its operational stability, the PEDOT-NFs/GOx-3 biosensor was tested by addition of 0.5 mM glucose. Fig. 8 shows that the current response of the PEDOT-NFs/GOx-3 nanofiber biosensor retained approximately 93.13% of its original response after 24 consecutive measurements. The standard deviation of the current response was found to be ± 0.0137 and the RSD% was found to be 2.96%. Such good operational stability of the PEDOT-NFs/GOx-3 biosensor could be due to the biocompatibility of the porous PEDOT nanofibers that could help to preserve the GOx molecules without the loss of its activity.⁴³



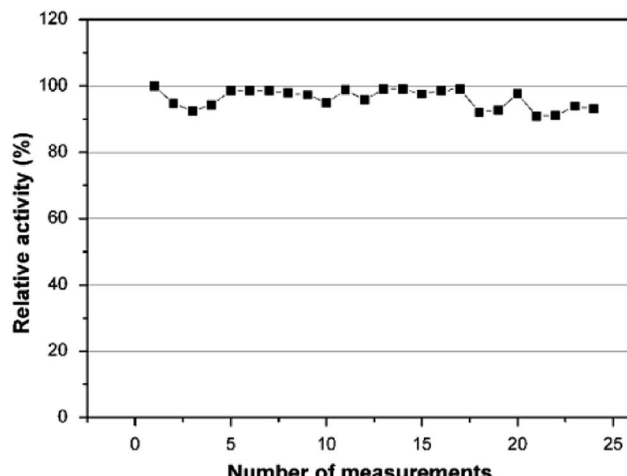


Fig. 8 Operational stability of the PEDOT-NFs/GOx-3 biosensor.

Amperometric studies on the PEDOT-NFs/GOx nanofiber biosensors based on oxygen consumption

Biosensors based on the measurement of peroxide formation have the advantage of being simpler. However, the main problem with these type of sensors is the requirement of a high operation potential for achieving high sensitivity. Many electroactive species, such as citric acid, sucrose, fructose and ascorbic acid (AA) are very common in beverages and foods. These species can be oxidized at a high potential and their signals can influence the selectivity of the biosensors. Since measuring the amount of hydrogen peroxide produced by the enzymatic reaction necessitates higher working potentials and could cause matrix over-oxidation, measuring the oxygen consumption is considered to be a viable, low working potential approach for the electrochemical sensing of glucose.

In order to see the full potential of the PEDOT-NFs/GOx nanofiber biosensors, we performed similar amperometric studies where the biosensors with different enzyme loadings (46.25 U GOx, 92.5 U GOx, 185 U GOx, 277.5 U GOx and 370 U GOx) were again constructed and investigated for their amperometric responses (at -0.6 V) to varying glucose concentrations.

For each biosensor, the calibration curves were plotted and the sensitivity, linear range and LOD, K_m and I_{max} values were determined. Table 2 summarizes the performances of the generated biosensors. Among the biosensors, PEDOT-NFs/GOx-2 (with 92.5 U GOx) displayed the highest sensitivity ($272.58 \mu\text{A mM}^{-1} \text{cm}^{-2}$) with a linear range of 0.01 – 0.6 mM. The biosensor retained approximately 87.1% of its original response after 15 consecutive measurements. In comparison to the literature, all of the biosensors revealed higher sensitivity with similar response times. Unfortunately, all of the biosensors exhibited a narrower linear detection range and lower operational stability, and lower K_m values compared to those based on hydrogen peroxide measurements.

Interference study

To determine the effects of interferents, 0.05 M (for 0.6 V) and 0.5 M (for -0.6 V) solutions of sucrose, fructose, citric acid and AA were prepared and sequentially injected into the electrochemical cell. In Fig. 9a and b, the amperometric signals of glucose, sucrose, fructose, citric acid and AA are shown. As can be seen, the typical interferents had an insignificant or no interference effect when compared to the well-defined signal of the glucose.^{44,45} Such results show the high selectivity of the PEDOT nanofiber based biosensors even in interferent rich environments.

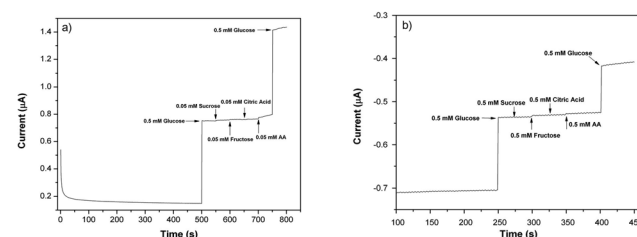


Fig. 9 Amperometric responses of (a) the PEDOT-NFs/GOx-3 (at 0.6 V) and (b) PEDOT-NFs/GOx-2 (at -0.6 V) nanofiber biosensors versus sucrose, fructose, citric acid and AA (0.1 M PBS, pH 6.5 , at 25 °C).

Table 2 Performances of all of the PEDOT-NFs/GOx nanofiber biosensors at -0.6 V

	PEDOT-NFs/GOx-1	PEDOT-NFs/GOx-2	PEDOT-NFs/GOx-3	PEDOT-NFs/GOx-4	PEDOT-NFs/GOx-5
Linear range	0.01 – 0.8 mM	0.01 – 0.6 mM	0.01 – 0.8 mM	0.04 – 1 mM	0.01 – 0.7 mM
Sensitivity ($\mu\text{A mM}^{-1} \text{cm}^{-2}$)	215.51	272.58	111.78	177.7	196.3
LOD (μM)	19.2	67.8	165	80	108
Stability	After the ninth use, 80.65%	After the fifteenth use, 87.1%	After the sixth use, 82.2%	After the eighth use, 75.1%	After the fifth use, 94.21%
Std. deviation	± 0.2121	± 0.116	± 0.174	± 0.345	± 0.055
RSD	9.4%	6.53%	9.13%	15.3%	3.3%
K_m (mM)	0.81	0.057	0.552	0.124	0.121
I_{max} (μA)	9.3	1.256	3.95	4.924	1.89
Response time (s)	1–2	2–3	2–3	50–52	120



Table 3 The glucose analyses of commercial beverages

Samples	Spectroscopy (HPLC) (g/100 ml)	PEDOT-NFs/GOx-3 biosensor (g/100 ml)	Recovery (%)
Cherry juice	4.471 ± 0.122	4.452 ± 0.055	99.6
Mixed fruit juice	3.261 ± 0.027	3.275 ± 0.017	100.42

Determination of glucose in real samples

The amount of glucose in real samples was determined using the PEDOT-NFs/GOx-3 biosensor for several beverages. In these analyses, cherry juice and mixed fruit juice were directly added into the buffer (0.1 M PBS, pH = 6.5) without any dilution. 10 µl of fruit juice was used in every addition and the related current changes were recorded, which were then correlated to the analyte concentration through the available calibration curves. The corresponding results, which are the average of 3 consecutive measurements, and the data from the HPLC analysis are shown in Table 3. As can be seen, the biosensor is capable of measuring real samples with a high percentage recovery.

Conclusions

In this study, bead free, homogeneous nanofibers of PEDOT were produced *via* a two-step procedure where FeCl₃-containing electrospun PAN nanofiber mats were subjected to chemical vapor polymerization in the presence of EDOT. The nanofibers were characterized by SEM, FTIR spectroscopy, and CV studies, which revealed the homogeneous coating of electroactive PEDOT on the PAN nanofibers.

Fabrication of the biosensors was achieved through the loading of various amounts of GOx on the PEDOT nanofibers, which were then entrapped by glutaraldehyde. The biosensors were used for both hydrogen peroxide production and oxygen consumption measurements. For each biosensor the current response (ΔI) *versus* glucose concentrations (mM) calibration curves were plotted and the sensitivity, linear range and LOD, K_m (mM) and I_{max} (µA) values were determined and the stabilities of all of the sensors were investigated. Our studies have shown that the biosensors operating at higher potentials (based on hydrogen peroxide production) generally revealed lower LOD values with a wider linear range, higher stability and good sensitivity. Among these, the PEDOT-NFs/GOx-3 nanofiber biosensor showed good sensitivity (74.22 µA mM⁻¹ cm⁻²) and LOD (2.9 µM) with a response time of 2–3 s in 6.5 pH at an operating potential of 0.6 V. The sensor retained approximately 93% of its original response after 24 consecutive measurements with a RSD value of 2.96%. The PEDOT-NFs/GOx-2 nanofiber biosensor showed a remarkable sensitivity of 272.58 µA mM⁻¹ cm⁻² with a LOD of 67.8 µM in 6.5 pH at –0.6 V. Despite the very high sensitivity (111.78 µA mM⁻¹ cm⁻² to 272.58 µA mM⁻¹ cm⁻²) of the biosensors operating at –0.6 V, unfortunately all failed to have suitable operational stability. Our studies have shown that the increase in the amount of enzyme loading had an adverse effect on the response time, which might be related to the excessive swelling of the PEDOT nanofibers that was

observed in the SEM images. PEDOT-NFs/GOx-3 (at 0.6 V and –0.6 V) showed no interference effects to common interferents such as sucrose, fructose, citric acid and AA, that are found in beverages. Finally, the biosensor was successfully utilized in real sample analyses, also indicating the reliability of these nanofibers.

In this study, we were able to present a simple, low cost (without using gold, Pd nanoparticles, *etc.*), robust approach for the production of PEDOT nanofiber biosensors using simple electrospinning and chemical vapor polymerization techniques. The sensors generally revealed good sensitivity, LOD and operational stability, highly comparable to those found in literature. The adopted methodology might be the first in line to open up a new avenue, making these interference-free PEDOT sensors viable candidates for commercialization. Further studies are underway to construct tyrosinase sensors that could be used for the detection of phenolic compounds.

Conflicts of interest

There are no conflicts to declare.

Acknowledgements

We are grateful to the Akdeniz University Research Fund (FBA-2017-2516) for supporting this study.

Notes and references

- 1 A. Senthamilan, B. Balusamy and T. Uyar, *Anal. Bioanal. Chem.*, 2015, **408**, 1285.
- 2 A. Kros, N. A. J. M. Sommerdijk and R. J. M. Nolte, *Sens. Actuators, B*, 2005, **106**, 289.
- 3 H. Hosseini, S. J. T. H. Rezaieb, P. Rahmania, R. Sharifia, M. R. Nabida and A. Bagheri, *Sens. Actuators, B*, 2014, **195**, 85.
- 4 B. L. Groenendaal, F. Jonas, D. Freitag, H. Pielartzik and J. R. Reynolds, *Adv. Mater.*, 2000, **12**, 481.
- 5 L. Zhang, X. Duana, Y. Wenb, J. Xub, Y. Yaob, Y. Luab, L. Lub and O. Zhang, *Electrochim. Acta*, 2012, **72**, 179.
- 6 M. Liu, Y. Wen, J. Xu, H. He, D. Li, R. YUE and G. Liu, *Anal. Sci.*, 2011, **27**, 477.
- 7 G. Yang, K. L. Kampstra and M. R. Abidian, *Adv. Mater.*, 2014, **26**, 4954.
- 8 P. Santhosh, K. M. Manesh, S. Uthayakumar, S. Komathi, A. I. Gopalan and K. P. Lee, *Bioelectrochemistry*, 2009, **75**, 61.
- 9 M. J. Hampden-Smith and T. T. Kodas, *Chem. Vap. Deposition*, 1995, **1**, 8.
- 10 M. Kumar and Y. Ando, *J. Nanosci.*, 2010, **10**, 3739.

11 G. Che, B. B. Lakshmi, C. R. Martin, E. R. Fisher and R. S. Ruoff, *Chem. Mater.*, 1998, **10**, 260.

12 A. Laforgue and L. Robitaille, *Chem. Mater.*, 2010, **22**, 2474.

13 M. Z. Çetin and P. Camurlu, *J. Electrochem. Soc.*, 2017, **164**, 585.

14 A. Ramanavicius, A. Kausaite and A. Ramanaviciene, *Sens. Actuators, B*, 2005, **111–112**, 532.

15 A. Shrivastava, V. Gupta and R. Article, *Chron. Young Sci.*, 2011, **2**, 21.

16 A. Laforgue and L. Robitaille, *Polym. Prepr.*, 2008, **49**, 624.

17 Z. Zhou, X.-F. Wu, Y. Ding, M. Yu, Y. Zhao, L. Jiang, C. Xuan and C. Sun, *J. Appl. Polym. Sci.*, 2014, **131**, 1.

18 W. X. Zhang, Y. Z. Wang and C. F. Sun, *J. Polym. Res.*, 2007, **14**, 467.

19 M. Wu, Q. Wang, K. Li, Y. Wu and H. Liu, *Polym. Degrad. Stab.*, 2012, **97**, 1511.

20 X. Zhang, Y. Huang and P. Liu, *Nano-Micro Lett.*, 2016, **8**, 131.

21 P. Damlin, C. Kvarnstrom and A. Ivaska, *J. Electroanal. Chem.*, 2004, **570**, 113.

22 C. Kvarnstrijms, H. J. Ahonen and J. Kankarec, *Synth. Met.*, 1999, **101**, 66.

23 C. Ocampo, R. Oliver, E. Armelin, C. Alemán and F. Estrany, *J. Polym. Res.*, 2006, **13**, 193.

24 B. Duran, M. C. Turhan, G. Bereket and A. S. Saraç, *Electrochim. Acta*, 2009, **55**, 104.

25 A. Laforgue and L. Robitaille, *Macromolecules*, 2010, **43**, 4194.

26 A. Laforgue, *J. Power Sources*, 2011, **196**, 559.

27 A. N. Aleshin, *Adv. Mater.*, 2006, **18**, 17.

28 M. G. Han and S. H. Foulger, *Small*, 2006, **2**, 1164.

29 T. H. Lee, K. Do, Y. W. Lee, S. S. Jeon, C. Kim, J. Kob and S. S. Im, *J. Mater. Chem.*, 2012, **22**, 21624.

30 J. L. Duvail, P. Retho, S. Garreaua, G. Louarna, C. Godona and S. D. Champagne, *Synth. Met.*, 2002, **131**, 123.

31 J. Grobelny, M. Sok and E. Turska, *Eur. Polym. J.*, 1988, **24**, 1195.

32 K. N. Layton and M. R. Abidian, *2011 5th Int. IEEE/EMBS Conf. Neural Eng. NER 2011*, 2011, pp. 298–301.

33 B. Piro, L. A. Dang, M. C. Pham, S. Fabiano and C. Tran-Minh, *J. Electroanal. Chem.*, 2001, **512**, 101–109.

34 P. C. Nien, T. S. Tung and K. C. Ho, *Electroanalysis*, 2006, **18**, 1408–1415.

35 X. Xiao, M. Wang, H. Li and P. Si, *Talanta*, 2013, **116**, 1054–1059.

36 P. A. Palod and V. Singh, *Sens. Actuators, B*, 2015, **209**, 85–93.

37 C. Guo, L. Zhou and J. Lv, *Polym. Polym. Compos.*, 2013, **21**, 449–456.

38 C. Chen, Q. Xie, D. Yang, H. Xiao, Y. Fu, Y. Tan and S. Yao, *RSC Adv.*, 2013, **3**, 4473–4491.

39 G. Rahman and S. A. Mian, *Int. J. Biosen. Bioelectron.*, 2017, **3**, 00051.

40 Z. G. Zhu, L. Garcia-Gancedo, A. J. Flewitt, H. Q. Xie, F. Moussy and W. I. Milne, *Sensors*, 2012, **12**, 5996–6022.

41 M. M. Rahman, A. J. S. Ahammad, J. H. Jin, S. J. Ahn and J. J. Lee, *Sensors*, 2010, **10**, 4855–4886.

42 A. S. Rad, A. Mirabi, E. Binaian and H. Tayebi, *Int. J. Electrochem. Sci.*, 2011, **6**, 3671–3683.

43 X. Su, J. Wei, X. Ren, L. Li, X. Meng, J. Ren and F. Tang, *J. Biomed. Nanotechnol.*, 2013, **9**, 1776.

44 R. Thota and V. Ganesh, *Analyst*, 2014, **139**, 4661.

45 W. Jia, M. Guo, Z. Zheng, T. Yu, E. G. Rodriguez, Y. Wang and Y. Lei, *J. Electroanal. Chem.*, 2009, **625**, 27.

